JGR Space Physics

RESEARCH ARTICLE
10.1029/2020JA028909

Key Points:

- Large wind disturbances are observed at ~80–98 km altitude ~60°S by three meteor radars during the 2019 Antarctic stratospheric warming
- A quasi 6-day oscillation is observed at different longitudes indicating the presence of the westward propagating zonal wave-1 wave
- This study provides observational evidence of the nonlinear interaction between the 6-day planetary wave and the semidiurnal tide

Supporting Information:

Supporting Information may be found in the online version of this article.

Correspondence to:

G. Liu,
guiping@berkeley.edu

Citation:

Liu, G., Janches, D., Lieberman, R. S., Moffat-Griffin, T., Mitchell, N. J., Kim, J.-H., & Lee, C. (2021). Wind variations in the mesosphere and lower thermosphere near 60°S latitude during the 2019 Antarctic sudden stratospheric warming. *Journal of Geophysical Research: Space Physics*, *126*, e2020JA028909. https://doi.org/10.1029/2020JA028909

Received 3 NOV 2020
Accepted 24 APR 2021

Wind Variations in the Mesosphere and Lower Thermosphere Near 60°S Latitude During the 2019 Antarctic Sudden Stratospheric Warming

Guiping Liu[1,2,3], Diego Janches[3], Ruth S. Lieberman[3], Tracy Moffat-Griffin[4], Nicholas J. Mitchell[4,5], Jeong-Han Kim[6], and Changsup Lee[6]

[1]Space Sciences Laboratory, University of California, Berkeley, Berkeley, CA, USA, [2]CUA/NASA GSFC, Greenbelt, MD, USA, [3]Heliophysics Science Division, ITM Physics Laboratory, NASA Goddard Space Flight Center, Greenbelt, MD, USA, [4]British Antarctic Survey, Cambridge, UK, [5]Centre for Space, Atmospheric and Oceanic Science, University of Bath, Bath, UK, [6]Department of Polar Climate Science, Korea Polar Research Institute, Incheon, South Korea

Abstract Sudden stratospheric warmings (SSWs) could act as an important mediator in the vertical coupling of atmospheric regions and dramatic variations in the mesosphere and lower thermosphere (MLT) in response to SSWs have been documented. However, due to rare occurrences, SSWs in the Southern Hemisphere (SH) and their impacts on the MLT dynamics are not well understood. This study presents an analysis of MLT winds at ~80–98 km altitudes measured by meteor radars located at Tierra del Fuego (53.7°S, 67.7°W), King Edward Point (54.3°S, 36.5°W) and King Sejong Station (62.2°S, 58.8°W) near 60°S latitude during the Antarctic winter. Eastward zonal winds from these stations are observed to decrease significantly near the peak date of the 2019 Antarctic SSW, and both zonal and meridional winds in 2019 exhibit considerable differences to the mean winds averaged over other non-SSW years. A quasi 6-day oscillation is observed at all three radar locations, being consistent with the presence of the westward propagating zonal wave-1 planetary wave. The vertical wavelength of this wave is estimated to be ~55 km, and the enhancement of the wave amplitude during this SSW is noticeable. Evidence of the interaction between the 6-day wave and the semidiurnal diurnal tide is provided, which suggests a possible mechanism for SSWs to impact the upper atmosphere. This study reports the large-scale variations in winds in the MLT region at SH midlatitudes to high latitudes in a key dynamic but largely unexplored latitudinal band in response to the 2019 Antarctic SSW.

Plain Language Summary Sudden stratospheric warmings (SSWs) manifest dynamic disruptions in the polar winter stratosphere, characterized as rapid changes in temperature and wind within a few days. Although SSWs are by definition a stratospheric phenomenon, they have significant impacts throughout the middle and upper atmosphere. Many studies of the SSW impacts on the mesosphere and lower thermosphere (MLT) have been performed, mostly for the Northern Hemisphere (NH). In the Southern Hemisphere (SH), SSW events are rare and thus the Antarctic SSWs are not well known. An unusual SSW occurred in the SH during September 2019, and the work presented here focuses on studying the MLT winds observed by three meteor radars located at Tierra del Fuego (53.7°S, 67.7°W) in Argentina, King Edward Point (54.3°S, 36.5°W) on South Georgia Island, and King Sejong Station (62.2°S, 58.8°W) in King George Island. These observations are over a key dynamic but largely unexplored region around the Drake Passage. This study presents the large-scale variations in the MLT winds at SH midlatitudes to high latitudes which are believed to be in response to the 2019 Antarctic SSW. Possible mechanisms for SSWs to impact the upper atmosphere are discussed.

1. Introduction

Sudden stratospheric warmings (SSWs) are dramatic meteorological events, which are characterized as a sharp rise in temperature by tens of degrees Kelvin within a few days in the winter polar stratosphere (e.g., Andrews et al., 1987). Accompanying the temperature increase, the stratospheric circulation undergoes a substantial change as westerly (eastward) winds are decelerated and during major warmings, the polar vortex is almost entirely broken down and replaced by easterly (westward) winds (e.g., Butler et al., 2015). Minor warmings are defined if the zonal mean zonal wind at 10 hPa (~30 km) only decelerates and does

not completely reverse. SSWs do not occur every winter, and typically six major warmings occur in a decade in the Northern Hemisphere (NH) (Charlton & Polvani, 2007). SSWs are driven by upward propagating stationary planetary waves that are forced in the troposphere by land-sea heating contrasts and orography (e.g., Matsuno, 1971). Due to weak planetary wave forcing, SSWs rarely occur in the Southern Hemisphere (SH) (e.g., Chandran et al., 2014). The 2002 event is the only major SSW that has ever been observed at high-southern latitudes (e.g., Krüger et al., 2005). Minor warming events have occurred recently in the SH during the 2010 and 2019 Antarctic winter (e.g., Eswaraiah et al., 2016; Stober et al., 2020).

SSWs are by definition a polar stratospheric phenomenon, but they have impacts over a wide range of latitudes throughout the mesosphere and lower thermosphere (MLT) and the ionosphere (e.g., Chau et al., 2012; Eswaraiah et al., 2016; Fejer et al., 2011; Goncharenko et al., 2010, 2012, 2020; Jacobi et al., 2003; Lin et al., 2020; Liu & Roble, 2002; Oberheide et al., 2020; Pedatella et al., 2010, 2018; Pedatella, Liu, Richmond, et al., 2012; Yamazaki et al., 2020). By modulating tides, planetary waves could extend their influences into low latitudes and midlatitudes at high altitudes (e.g., G. Liu et al., 2010; H.-L. Liu et al., 2010). Global responses of migrating diurnal, semidiurnal, and terdiurnal tides to SSWs in the MLT region have all been extensively documented (e.g., Fuller-Rowell et al., 2010; Hibbins et al., 2019; Jin et al., 2012; Lieberman et al., 2004; Pedatella, Liu, Richmond, et al., 2012; Pedatella & Liu, 2013; Wang et al., 2011). Modeling studies have shown that tidal amplitudes increase with the changes of zonal mean zonal winds (e.g., Jin et al., 2012; Pedatella, Liu, Richmond, et al., 2012) and stratospheric ozone variations (e.g., Goncharenko et al., 2012; Siddiqui et al., 2019). The nonlinear interaction of migrating tides with planetary waves could generate nonmigrating tides, causing enhancements of tidal amplitudes (e.g., Angelats i Coll & Forbes, 2002; Chang et al., 2009; Lieberman et al., 2015; Pancheva et al., 2009; Pedatella, Liu, Richmond, et al., 2012; Teitelbaum & Vial, 1991). Additionally, amplifications of semidiurnal lunar tides resulting from the zonal mean changes in the atmosphere have been reported (Forbes & Zhang, 2012; Pedatella et al., 2013). Through various processes, SSWs can impact the dynamics of the middle and upper atmosphere over the globe. However, the actual perturbations during SSWs are complex and several processes combined may be involved (Pedatella & Liu, 2013). More work is needed to fully explain the MLT variations and how exactly SSWs impact the upper atmosphere.

Studies of the SSW impacts have focused on the NH, and there are only limited investigations of the Antarctic SSW in SH winter. These mostly include the 2002 major warming and the 2010 minor warming events, and multi-day oscillations with periods ~14–16 days were observed in the MLT region during both events (e.g., Dowdy et al., 2004; Eswaraiah et al., 2016, 2018). Most recently, an unusual SSW driven by exceptionally strong planetary wave activity occurred in the SH during September 2019 (e.g., Stober et al., 2020; Yamazaki et al., 2020). Although this SSW is categorized as a minor warming event, it features a very large temperature increase of ~50 K at ~30 km altitude over the South pole. A quasi 6-day oscillation has been identified in the equatorial ionosphere, and it has been attributed to the forcing by the 6-day wave propagating from the stratosphere (e.g., Goncharenko et al., 2020; Lin et al., 2020; Yamazaki et al., 2020). The 6-day planetary waves (PWs) have been recognized as important drivers of the ionospheric variability (e.g., Forbes et al., 2018; Gu et al., 2018; Yamazaki, 2018). However, the PW propagations and their impacts on the SH mid-to-high latitude MLT dynamics during this 2019 Antarctic SSW have not been well studied.

The mid-to-high latitude range in the SH encompasses the Southern Andes, the Drake Passage, and the Antarctic Peninsula, where the most dramatic motions of the atmosphere occur (e.g., Alexander et al., 2008; Eckermann et al., 2006; Jiang et al., 2002; Preusse et al., 2006; de Wit et al., 2017). This range covers the well-known World's hotspot of topography-generated gravity waves and the observations have revealed large stratospheric gravity wave (GW) activity over the Drake Passage. Yet, parameterizations of GWs in general circulation models are generally not accurate (e.g., Garcia et al., 2017). The modeled zonal winds in the MLT region normally have large discrepancies at ~60°S latitudes because the breaking of very strong mountain waves over the Southern Andes and the Antarctic Peninsula is not sufficiently simulated (e.g., Becker & Vadas, 2018). Nonpolar orbiting satellites do not always observe midlatitudes to high latitudes during every yaw cycle and at most two local times are sampled per day. Ground-based observations can be continuous in time, but they have limited coverages to certain locations. Observations of SH midlatitudes to high latitudes are thus relatively sparse, and this region remains largely unexplored (e.g., Stober et al., 2020).

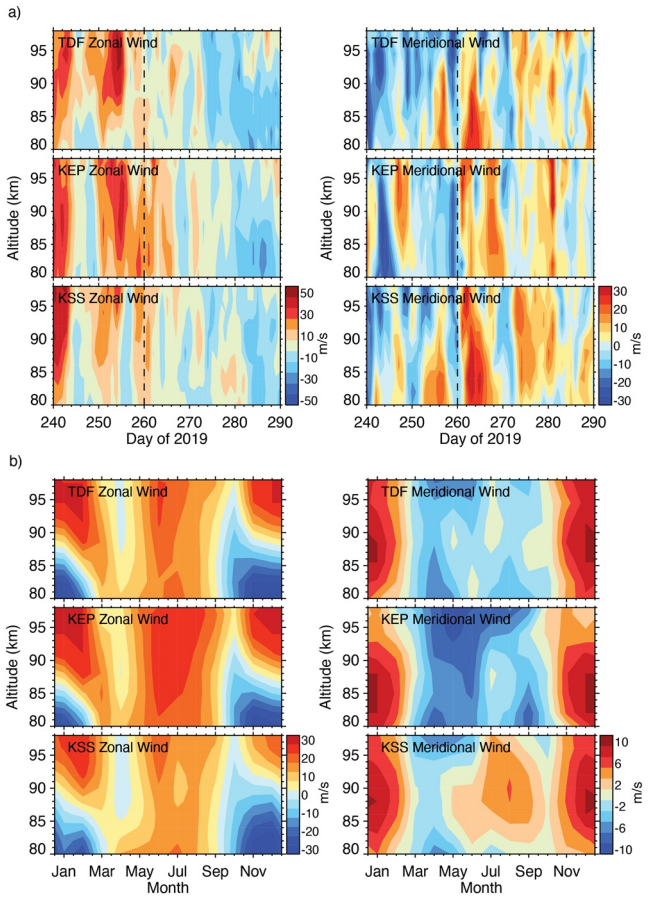

Figure 1. (a) Daily mean zonal and meridional winds measured by the meteor radars at TDF, KEP, and KSS for the altitude range of ~80–98 km during Days 240–290 of 2019 (August 28–October 17). The vertical dashed line marks the peak date of the 2019 Antarctic SSW on September 17 (Day 260). (b) Monthly mean zonal and meridional winds averaged over 2016–2018 at the three radar locations.

The MLT winds have been measured near 60°S latitude by three meteor radars at Rio Grande, Tierra del Fuego (TDF; 53.7°S, 67.7°W) in Southern Argentina, King Edward Point station (KEP; 54.3°S, 36.5°W) on South Georgia Island, and King Sejong Station (KSS; 62.2°S, 58.8°W) on King George Island on the Northern tip of the Antarctic Peninsula. These meteor radar winds allow us to identify the wave activities and large-scale variations in the MLT region in this key dynamic but largely unexplored area (e.g., Eswaraiah et al., 2016; Fritts et al., 2019; Iimura et al., 2015; Lee et al., 2013; G. Liu et al., 2020; de Wit et al., 2017). The radar wind measurements also allow us to assess the impacts of the 2019 Antarctic SSW on the MLT dynamics during the SH winter (e.g., Stober et al., 2020).

2. Observations

2.1. Meteor Radar Winds

The all-sky interferometer meteor radars have been operated at TDF, KEP, and KSS, and all employ the same system to measure the MLT wind field at high resolutions (e.g., Eswaraiah et al., 2016; Fritts et al., 2010; Kim et al., 2010; Lee et al., 2013). Zonal and meridional winds at ~3 km altitude bins in the range from ~80 to 98 km are obtained, and this study uses the hourly mean winds measured over the years from 2016 to 2019 at the three sites. These wind data are almost continuous except that there are occasional data gaps. At KEP, the data are missing for a few days in early July and mid-November of 2019. These occur many days before or after the 2019 Antarctic SSW that peaks around September 17 (Day 260). Data available are thus sufficient for the analysis of the SSW impacts.

Figure 1a shows the daily averaged zonal and meridional winds at the three stations from August 28–October 17 of 2019 covering the SSW event. The MLT winds over these different locations exhibit a similar pattern across the vertical range for both wind components. The zonal components are dominated by the eastward winds during June–September in winter (see Figure 1b), and near the peak SSW warming in mid-September of 2019, the eastward winds decrease almost simultaneously at all stations from ~50 m s^{-1} to be only few m s^{-1} or even reverse the directions. The weak eastward winds persist for a few days, and then in early October 2019, the wind reverses to be mostly westward continuing into summer below ~85 km altitude. The large decrease of eastward winds during this 2019 SSW appears to correspond to the stratospheric wind change. The meridional winds are observed to be relatively weak with the largest daily mean values of only ~30 m s^{-1}, and the wind reversals often occur throughout the winter season. Given the latitudinal and longitudinal differences of these radar stations, the wind variations observed during the 2019 SSW constitute a large-scale signature.

Large disturbances related to the SSW are evident in Figure 2, which compares the 2019 winds with the average winds from other years of 2016–2018. Note there is no SSW occurring in the SH during 2016–2018. Time series of the daily mean winds during July–November observed at an altitude ~91 km by the three radars are shown. For all of the three radar stations, the winds in 2019 exhibit considerable departures from the multiyear averages. The differences are seen in the zonal winds, and around day 253 about a week before the SSW peak, the eastward zonal winds over TDF and KEP are observed to be significantly larger than the averaged values by ~10–30 m s^{-1}. Subsequently, these zonal winds largely decrease during the SSW peak, barely recognizable flowing in the eastward direction. Meanwhile, the meridional winds in 2019 are also observed to deviate from the multi-year averaged values and the winds at the three stations all turn into large northward (equatorward) winds following the SSW peak. Simulations from a general circulation model have shown that on the day of the peak SSW, the circulation at 90–105 km altitudes changes to be equatorward and upward for midlatitudes to high latitudes (Liu and Roble, 2002). The meridional winds

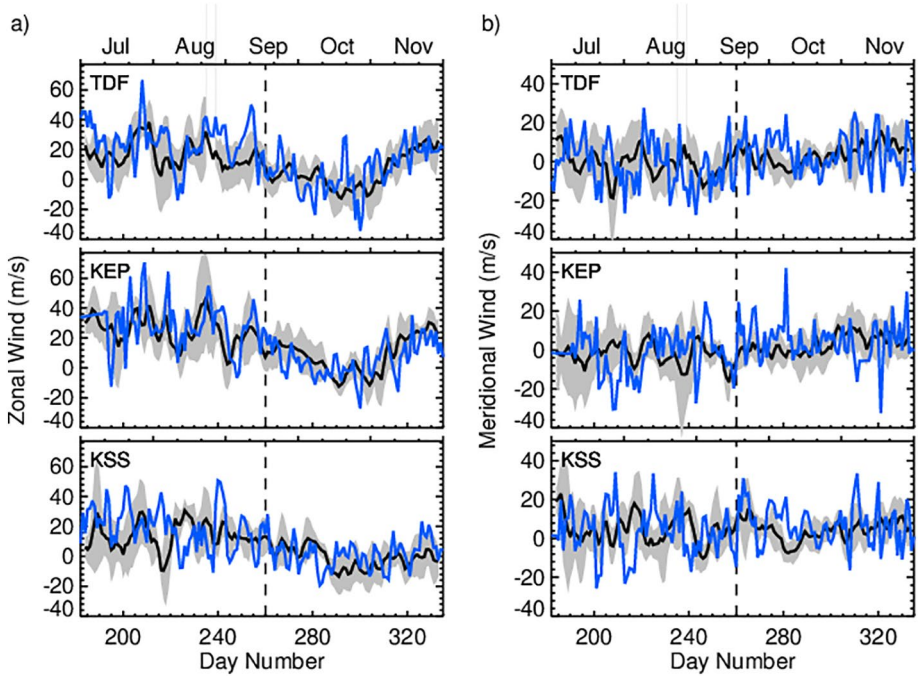

Figure 2. Daily averaged zonal and meridional winds measured at ~91 km altitude during July–November by three meteor radars. The blue curves represent the winds for 2019, and the black curves represent the values averaged over all other years from 2016–2018 (one standard deviation of the averages is denoted by the gray shade). The vertical dashed line marks the 2019 SSW peak date.

observed over the three radar locations are thus consistent with the modeled circulation change. Figure 2 also reveals large wave oscillations with short multiday periods in both zonal and meridional winds during this 2019 SSW event.

2.2. Quasi 6-Day Wave

Figure 3 shows the wavelet spectra of the zonal and meridional winds observed at ~91 km altitude by all three radars during July 1–November 30, 2019. Short-period waves above the 80% confidence level are observed, and around the peak SSW, the dominant wave observed has a period ~6 days in both wind components. This 6-day wave appears to be sporadic with the largest amplitudes detected during September 17–27 (Days 260–270). The wave is observed to occur at almost the same times between these radar locations, and the spectral patterns of TDF and KEP are much similar to each other than to KSS. This may be related to the large zonal (longitudinal) structure of the wave as TDF and KEP are located at similar latitudes and their longitudinal differences are relatively small. KSS is at a higher latitude than TDF and KEP, and the spectral difference may also be due to the latitudinal structure of the wave as the wave amplitude decreases over KSS. The presence of the 6-day wave signature is also noticeable in July and October/November. This is not surprising as the wave occurrence in the MLT region can be affected by several factors including the wave source, mean wind, instability, and the critical layers of the wave (e.g., H.-L. Liu et al., 2004). Previous studies have suggested that the 6-day wave amplitude may also be enhanced when the winter jet changes, or reverses, in the stratosphere and/or the mesosphere during the SSW event (e.g., H.-L. Liu et al., 2004).

The 6-day period observed in both zonal and meridional winds by the radars is indicative of a 6-day PW. Other properties of the wave, such as its zonal wavenumber can be determined using the three radars at various longitudes. Figure 4a shows the daily mean values of the meridional winds averaged over the vertical range from ~80 to 98 km during September 12–October 8 (Days 255–281) of 2019 when the 6-day wave is observed. The amplitude and phase of this 6-day wave are obtained through a least-squares fit (the daily mean winds are fitted to the 6-day wave as represented by the colored curves). The wave amplitude is observed to change slightly between different stations, having a smaller value of ~10 m s^{-1} at KSS than at

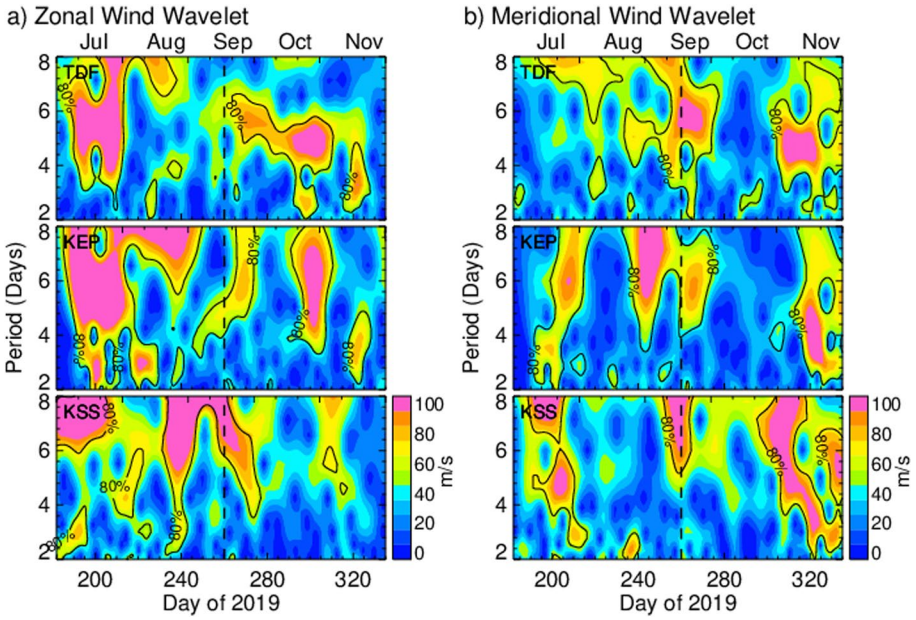

Figure 3. Wavelet spectra of hourly zonal and meridional winds observed at ~91 km altitude by three radars during July 1–November 30, 2019. The black contour line represents the 80% confidence interval. The vertical dashed line marks the 2019 SSW peak.

TDF and KEP. KSS is at a higher latitude and this amplitude difference is as expected given that this 6-day wave has been shown to be symmetric with respect to the Equator and the wave amplitude peaks at ±45° latitude (e.g., Yamazaki et al., 2020). Moreover, the fitting to the 6-day wave for KSS is not as good as for TDF and KEP, which could also be caused by the wave amplitude decrease over this site. Figure 4b examines the wave phases observed by the three radars, and the phases of the 6-day wave are plotted in relation to the longitudes of these radar locations. The phase change (slope) with respect to the longitude matches a westward propagating zonal wavenumber-1 planetary wave. This feature is again consistent with the 6-day PW that has been reported by previous studies (e.g., Lieberman et al., 2003; Yamazaki et al., 2020). It is worth noting that this phase calculation is based upon the wind observations averaged over a wide range of altitudes from ~80 to 98 km. This indicates that the vertical wavelength of the wave must be longer than this vertical range. Indeed, the 6-day PW has been identified to have a long vertical wavelength of ~60 km (e.g., Lieberman et al., 2003).

Using the phase change with altitude, it is possible to estimate the vertical wavelength of this 6-day PW. Figures 5a–5f show the zonal winds observed over TDF for altitudes across ~82–97 km, filtered for 5.5–6.5 day signatures. The crests of the wave (shown by colored dots) represent the progression of the wave's phase with altitude as plotted in Figure 5g. From the slope of this straight line, the vertical wavelength is determined to be ~50–60 km with the mean value of 55 km considering the uncertainties in the wave period and least-squares fit. Such a long vertical wavelength suggests that this wave could propagate upward into higher altitudes. It has been shown that the vertically propagating 6-day PW achieves large amplitudes in the lower thermosphere and through the zonal wind perturbations this wave drives the same periodic variations in the equatorial ionosphere (e.g., Yamazaki et al., 2020). The corresponding ionospheric variations have been reported (e.g., Goncharenko et al., 2020; Lin et al., 2020; Yamazaki et al., 2020). Our study provides a verification of the 6-day PW in the MLT region and suggests the potential impact of this wave for the ionospheric variability.

Figure 6 compares the 6-day wave amplitudes in 2019 with the average wave amplitudes from 2016 to 2018 observed at ~91 km altitude by the three radars (Figure S2 shows the wave amplitudes during each of these years). The 2019 wave amplitudes are generally within one standard deviation of the multiyear averages. However, around the peak date of the 2019 SSW, the wave amplitudes are observed to be significantly larger than the average amplitudes. The wave enhancement appears to be the strongest in the meridional winds

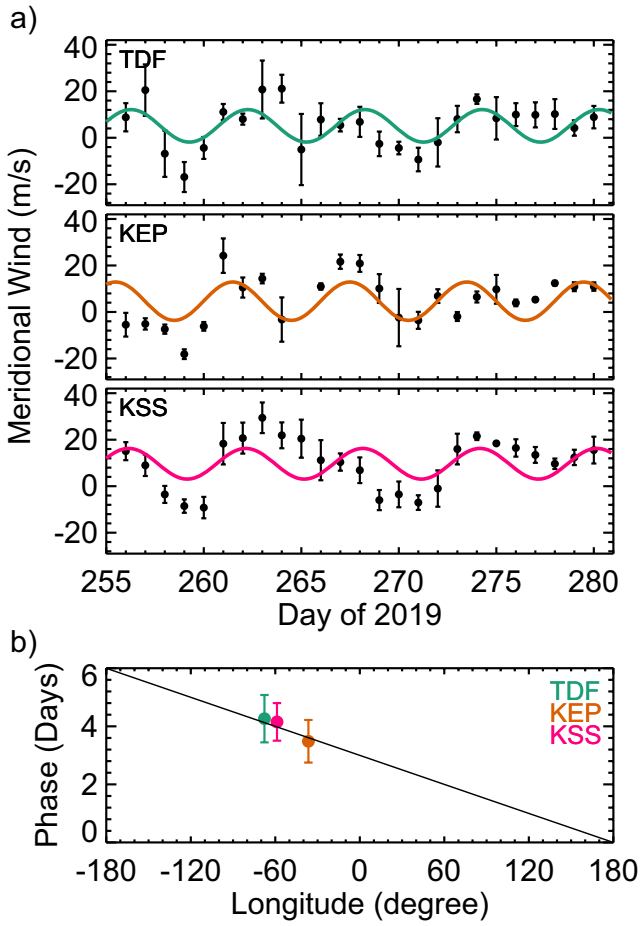

Figure 4. (a) Daily mean meridional winds averaged over the vertical range from ~80 to 98 km at the three radar locations during September 12–October 8, 2019 (Days 255–281). The vertical bar denotes one standard deviation of the averaged wind. The colored curve is from a least-squares fit to the 6-day wave. (b) Phase of the 6-day wave plotted versus longitude of the radar location. The colored bars represent the phase uncertainties from least-squares fit and also include the measurement uncertainties. The straight line has a slope equal to the phase speed of the westward propagating zonal wavenumber-1 planetary wave.

over TDF and KEP with the wave amplitudes being ~3 times greater than the averaged mean values. The enhancement is less evident over KSS, and again this could be due to the latitudinal change of this wave as the wave amplitude peaks at lower latitudes ~±45° (e.g., Yamazaki et al., 2020). The 6-day wave also reaches large amplitudes in the zonal wind components following the peak SSW although the amplitude departures from the multiyear averages are relatively smaller compared to those in the meridional winds. Both convection (Miyoshi & Hirooka, 1999) and baroclinic/barotropic instability (Lieberman et al., 2003; H.-L. Liu et al., 2004; Meyer & Forbes, 1997) can force the 6-day PW. A large wave forcing is induced during the 2019 SSW, and as such the 6-day wave is expected to reach a larger amplitude than the climatological mean value observed during other years without SSWs. Previous studies (e.g., Yamazaki et al., 2020) have proposed that this 6-day wave in September 2019 is most likely produced during unstable conditions from strong wind shear associated with stationary PW breaking. Due to baroclinic/barotropic instability, the wave grows rapidly by extracting energy from the unstable mean flow, and the reduced eastward mean flow and the weak wind reversal are favorable for the wave to propagate upward into high altitudes (Yamazaki et al., 2020). The wave amplification observed by the radars during the 2019 SSW is thus as expected.

2.3. Planetary Wave-Tide Interaction

The vertical wavelength of the 6-day PW identified (see Figure 5) during the 2019 SSW is close to that of semidiurnal tides and the semidiurnal tidal amplitude maximizes at ~60° latitude (e.g., Hagan et al., 1999; Hagan & Forbes, 2003). It could be possible that this 6-day wave interacts with these semidiurnal tides. Theory indicates that the nonlinear interaction between PWs and tides would generate two child (secondary) waves, whose frequencies and zonal wavenumbers are the sums and differences of the parent waves (e.g., Teitelbaum & Vial, 1991). Such an interaction could also produce a modulation of the tide with the period of the PW. As tides can propagate upward into higher altitudes, this modulation could act to extend the PW signature into the ionosphere (e.g., England et al., 2012; G. Liu et al., 2010; H.-L. Liu et al., 2010; G. Liu et al., 2015; Pancheva et al., 2002, 2009). The tide-PW interaction could thus be an important mechanism for the atmosphere-ionosphere coupling.

Figure 7a shows the periodograms of the hourly zonal and meridional winds at ~91 km altitude over TDF from September 21 to October 1 (Days 264–274) when the largest perturbations of the 6-day wave occur. Both the 6-day wave and the 12-h semidiurnal tide are observed in these winds. The red lines marked on the figure indicate the frequencies (13 and 11 h) that are the sums and the differences of the 6-day and 12-h wave frequencies, corresponding to the two child waves that would be produced by the nonlinear interaction between the 6-day wave and the semidiurnal tide. Of the two expected child waves, only the 13-h wave is observed above the 80% confidence level in both wind components. The vertical wavelength of this 13-h wave is estimated to be ~24 km using its phase change with altitude (see Figure S3). This shorter-vertical wavelength suggests that the 13-h child wave may not propagate as high altitudes as the 6-day wave. The 11-h wave is not seen and the reason for that is not known, but similar behavior has been reported before (e.g., England et al., 2012; Moudden & Forbes, 2010). Nonetheless, Figure 7a shows the direct detection of the 13-h child wave generated by the 6-day wave and the semidiurnal tide interaction in the MLT region using radar wind observations. This signature is also observed over KSS (see Figure S4).

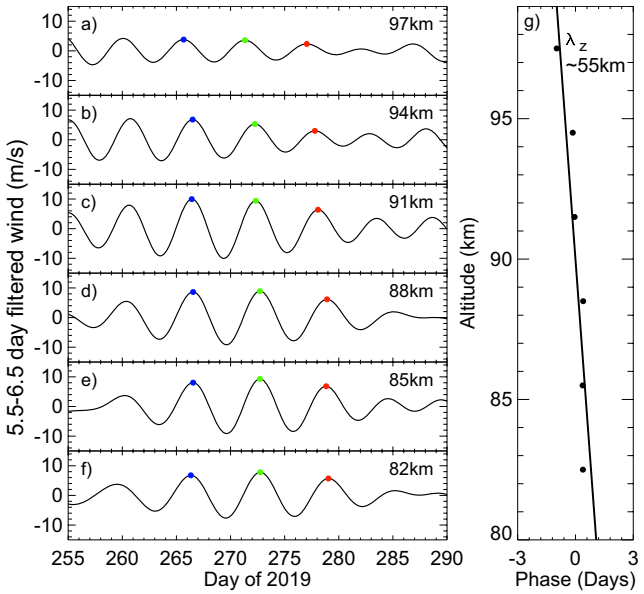

Figure 5. (a–f) 5.5–6.5 day bandpass filtered zonal winds over TDF at individual altitudes across ~82–97 km during September 12–October 17, 2019 (Days 255–290). The colored dots mark the maxima of the winds. (g) Phase of the 6-day wave as a function of altitude. The straight line is from the linear regression, and the slope of this line indicates the vertical wavelength of ~50–60 km assuming uncertainties of the wave period and least-squares fit.

Figure 7b shows the periodograms of the semidiurnal tidal amplitudes as a function of altitude in the range from ~80 to 98 km over TDF in the two wind components, using data from 28 August to 27 October (Days 240–300). Here a longer time interval is used to include enough data points for the spectral analysis. The analysis is performed separately at individual altitudes within the vertical range, and the consistency of signatures seen between adjacent altitude bins provides confidence in the result. A ~6-day periodicity is observed over the range from ~80 to 95 km in both zonal and meridional winds. The spectrum density peaks toward shorter periodicities than 6 days, and this is reasonable given that in Figure 7a the periodogram is also seen to peak over the shorter-period wave specifically for the zonal wind. This figure shows the interaction of the 6-day wave with the semidiurnal tide in the MLT region during this time. The periodicity appears below ~95 km, indicating that the interaction may occur over ~80–95 km altitude.

Modulation of tides has been generally accepted as the mechanism for SSWs to impact the ionospheric variability (e.g., Chau et al., 2012). Tidal variations are thought to relate to ozone changes caused by SSWs (e.g., Goncharenko et al., 2012; Siddiqui et al., 2019; Wu et al., 2011), changes in the zonal mean zonal winds that influence the vertical propagations of tides (e.g., Jin et al., 2012; Pedatella, Liu, Richmond, et al., 2012), and/or interactions with PWs (H.-L. Liu et al., 2010). This study provides observational evidence of the PW-tide interaction in the MLT region, and via this nonlinear interaction, the 6-days PW may indirectly affect the ionosphere at lower latitudes. Previous studies have shown that the 6-day wave could directly produce large zonal wind perturbations in the equatorial thermosphere (e.g., Miyoshi, 1999; Pedatella, Liu, & Hagan, 2012). Specifically, Yamazakai et al. (2020) have found that this 6-day wave in

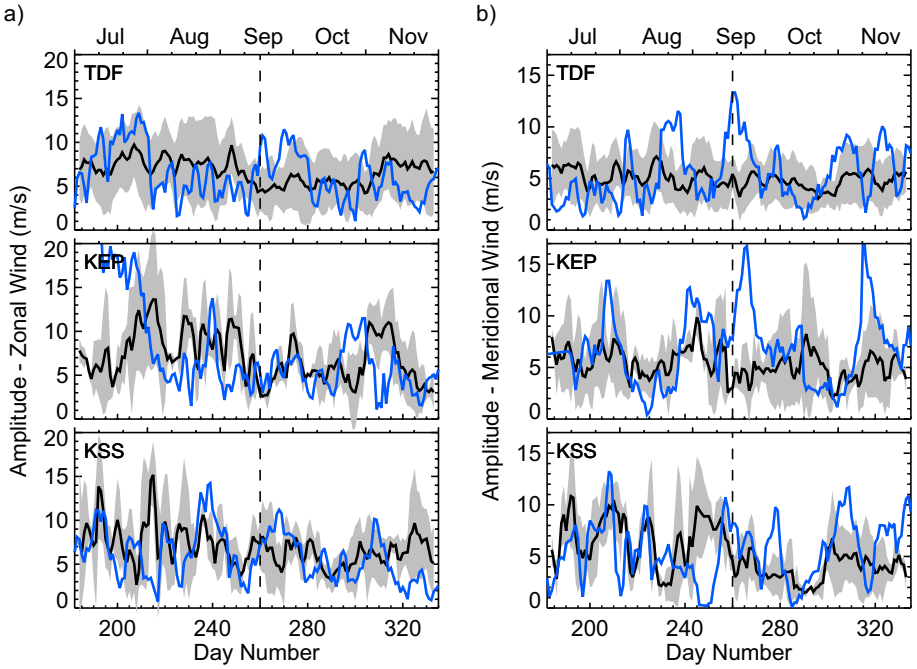

Figure 6. Daily amplitudes of the 6-day wave in the (a) zonal and (b) meridional winds at ~91 km altitude over three radar locations. The blue curve represents the amplitudes for 2019, and the black curve represents the averages from 2016 to 2018 (one standard deviation is denoted by the gray shade). The vertical dashed line marks the 2019 SSW peak.

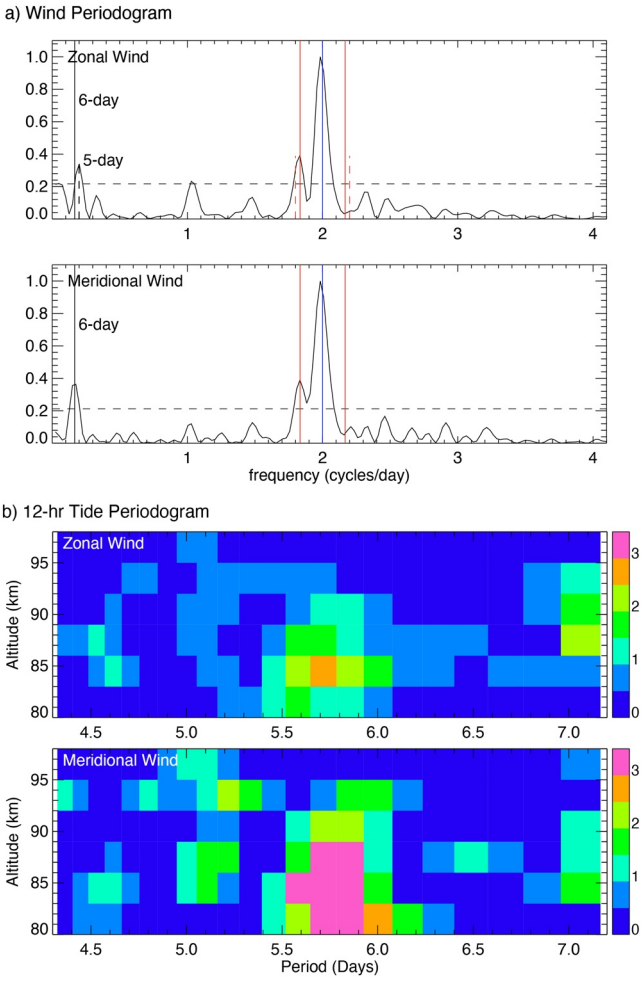

Figure 7. (a) Lomb-Scargle periodogram of the hourly zonal and meridional winds over TDF at ~91 km altitude during September 21–October 1 of 2019 (Days 264–274). The black vertical line marks the frequency of the 6-day wave, the blue line shows the frequency of the 12-h semidiurnal tide, and the red lines on the two sides mark the associated child waves assuming the nonlinear interaction between the 6-day wave and the semidiurnal tide. The vertical dashed lines for the zonal wind mark the frequencies of the 5-day wave and the corresponding child waves. The horizontal dashed line marks the 80% confidence level. (b) Lomb-Scargle periodogram of the 12-h tidal amplitudes in the vertical range from ~80 to 98 km in the zonal and meridional winds over TDF during August 28–October 27 of 2019 (Days 240–300).

the 2019 SSW propagates equatorward and upward from SH high latitudes. This study suggests that the 6-day PW interacts with the semidiurnal tide, so through both direct and indirect modulations, the wave could drive the ionospheric variations. However, a detailed study of the ionospheric variations and the relation to the 6-day wave is beyond the scope of this current study.

3. Summary

This study presents the zonal and meridional wind observations at ~80–98 km altitude by three meteor radars located at Tierra del Fuego (53.7°S, 67.7°W), King Edward Point (54.3°S, 36.5°W), and King Sejong Station (62.2°S, 58.8°W) near 60°S latitude in a key dynamic but largely unexplored region during the SH winter. These observations display a similar wind pattern in the vertical range, showing large variations in the MLT region in response to the 2019 Antarctic SSW. Strong eastward zonal winds are observed to decrease significantly while the meridional winds are turning into strong equatorward winds around the peak SSW warming, and both the zonal and meridional winds exhibit considerable differences to the mean winds averaged over other years without SSWs. These wind variations observed are overall consistent with the modeled circulation change in the MLT region during the SSW.

The three radar observations reveal a quasi 6-day oscillation, indicating the presence of the westward propagating zonal wave-1 PW. The wave is observed to propagate between these stations during the same time interval around the 2019 SSW peak, and the wave over TDF and KEP behaves more similarity to each other than to KSS. This may be related to the large zonal (longitudinal) structure of the wave as TDF and KEP are located at similar latitudes and their longitudinal differences are relatively small. The vertical wavelength is estimated to be ~55 km, and such a long vertical wavelength suggests that this wave could propagate upward into higher altitudes. Enhancement of the 6-day wave amplitude is also observed during the 2019 SSW event, suggesting the potential implications of this wave for the ionospheric variability.

This study provides observational evidence of the interaction between the 6-day PW and the semidiurnal diurnal tide, which suggests a possible mechanism for SSWs to impact the upper atmosphere. Through this nonlinear interaction, the 6-day wave may indirectly impact the ionosphere at lower latitudes. However, the detailed study of the ionospheric variations and their relation to the 6-day PW is beyond the scope of the current study and this should be investigated in a future study.

Data Availability Statement

The data used in this study are publicly available at http://millstonehill.haystack.mit.edu. The operation of the SAMMER radar at TDF is supported by NASA SSO program and NESC assessment T1-17-0120. The authors appreciate the invaluable support of Jose Luis Hormaechea, Carlos Ferrer, Gerardo Connon, Luis Barbero, and Leandro Mazlov with the operation of SAAMER. SAAMER operations are partially supported through a Memorandum of Understanding between the University of La Plata and the Catholic University of America.

Acknowledgments
Diego Janches, Ruth S. Lieberman, and Guiping Liu were supported by the NASA TIMED and ISFM Heliophysics programs. Guiping Liu was partially supported by NASA Grant 80NSSC18K0649 and 80NSSC20K1323. Jeong-Han Kim and Changsup Lee were supported by the Grant PE21020 from Korea Polar Research Institute.

References

Alexander, M. J., Gille, J., Cavanaugh, C., Coffey, M., Craig, C., Eden, T., et al. (2008). Global estimates of gravity wave momentum flux from high resolution dynamics limb sounder observations. *Journal of Geophysical Research*, *113*, D15S18. https://doi.org/10.1029/2007JD008807

Andrews, D. G., Leovy, C. B., & Holton, J. R. (1987). Middle atmosphere dynamics. Academic Press.

Angelats i Coll, M., & Forbes, J. M. (2002). Nonlinear interactions in the upper atmosphere: The s = 1 and s = 3 nonmigrating semidiurnal tides. *Journal of Geophysical Research*, *107*(A8), 3-1–3-15. https://doi.org/10.1029/2001JA900179

Becker, E., & Vadas, S. L. (2018). Secondary gravity waves in the winter mesosphere: Results from a high-resolution global circulation model. *Journal of Geophysical Research - D: Atmospheres*, *123*, 2605–2627. https://doi.org/10.1002/2017JD027460

Butler, A. H., Seidel, D. J., Hardiman, S. C., Butchart, N., Birner, T., & Match, A. (2015). Defining sudden stratospheric warmings. *Bulletin of the American Meteorological Society*, *96*, 1913–1928. https://doi.org/10.1175/BAMS-D-13-00173.1

Chandran, A., Collins, R. L., & Harvey, V. L. (2014). Stratosphere-mesosphere coupling during stratospheric sudden warming events. *Advances in Space Research*, *53*, 1265–1289. https://doi.org/10.1016/j.asr.2014.02.005

Chang, L. C., Palo, S. E., & Liu, H.-L. (2009). Short-term variation of the s = 1 nonmigrating semidiurnal tide during the 2002 stratospheric sudden warming. *Journal of Geophysical Research*, *114*, D03109. https://doi.org/10.1029/2008JD010886

Charlton, A. J., & Polvani, L. M. (2007). A new look at stratospheric sudden warmings. Part I: Climatology and modeling benchmarks. *Journal of Climate*, *20*, 449–469. https://doi.org/10.1175/jcli3996.1

Chau, J. L., Goncharenko, L. P., Fejer, B. G., & Liu, H.-L. (2012). Equatorial and low latitude ionospheric effects during sudden stratospheric warming events. *Space Science Reviews*, *168*(1–4), 385–417. https://doi.org/10.1007/s11214-011-9797-5

de Wit, R. J., Janches, D., Fritts, D. C., Stockwell, R. G., & Coy, L. (2017). Unexpected climatological behavior of MLT gravity wave momentum flux in the lee of the Southern Andes hot spot. *Geophysical Research Letters*, *44*, 1182–1191. https://doi.org/10.1002/2016GL072311

Dowdy, A. J., Vincent, R. A., Murphy, D. J., Tsutsumi, M., Riggin, D. M., & Jarvis, M. J. (2004). The large-scale dynamics of the mesosphere-lower thermosphere during the Southern Hemisphere stratospheric warming of 2002. *Geophysical Research Letters*, *31*, L14102. https://doi.org/10.1029/2004GL020282

Eckermann, S. D., Wu, D. L., Doyle, J. D., Burris, J. F., McGee, T. J., Hostetler, C. A., et al. (2006). Imaging gravity waves in lower stratospheric AMSU-A radiances, Part 2: Validation case study. *Atmospheric Chemistry and Physics*, *6*, 3343–3362. https://doi.org/10.5194/acp-6-3343-2006

England, S. L., Liu, G., Zhou, Q., Immel, T. J., Kumar, K. K., & Ramkumar, G. (2012). On the signature of the quasi-3-day wave in the thermosphere during the January 2010 URSI World Day Campaign. *Journal of Geophysical Research*, *117*, A06304. https://doi.org/10.1029/2012JA017558

Eswaraiah, S., Kim, Y. H., Hong, J., Kim, J.-H., Ratnam, M. V., Chandran, A., et al. (2016). Mesospheric signatures observed during 2010 minor stratospheric warming at King Sejong Station (62°S, 59°W). *Journal of Atmospheric and Solar-Terrestrial Physics*, *140*, 55–64. https://doi.org/10.1016/j.jastp.2016.02.007

Eswaraiah, S., Kim, Y. H., Lee, J., Ratnam, M. V., & Rao, S. V. B. (2018). Effect of Southern Hemisphere sudden stratospheric warmings on Antarctica mesospheric tides: First observational study. *Journal of Geophysical Research: Space Physics*, *123*, 2127–2140. https://doi.org/10.1002/2017JA024839

Fejer, B. G., Tracy, B. D., Olson, M. E., & Chau, J. L. (2011). Enhanced lunar semidiurnal equatorial vertical plasma drifts during sudden stratospheric warmings. *Geophysical Research Letters*, *38*, L21104. https://doi.org/10.1029/2011GL049788

Forbes, J. M., Maute, A., Zhang, X., & Hagan, M. E. (2018). Oscillation of the ionosphere at planetary-wave periods. *Journal of Geophysical Research: Space Physics*, *123*, 7634–7649. https://doi.org/10.1029/2018JA025720

Forbes, J. M., & Zhang, X. (2012). Lunar tide amplification during the January 2009 stratosphere warming event: Observations and theory. *Journal of Geophysical Research*, *117*, A12312. https://doi.org/10.1029/2012JA017963

Fritts, D. C., Iimura, H., Janches, D., Lieberman, R. S., Riggin, D. M., Mitchell, N. J., et al. (2019). Structure, variability, and mean-flow interactions of the January 2015 quasi-2-day wave at middle and high southern latitudes. *Journal of Geophysical Research - D: Atmospheres*, *124*, 5981–6008. https://doi.org/10.1029/2018JD029728

Fritts, D. C., Janches, D., Iimura, H., Hocking, W. K., Mitchell, N. J., Stockwell, R. G., et al. (2010). Southern Argentina Agile Meteor Radar: System design and initial measurements of large-scale winds and tides. *Journal of Geophysical Research*, *115*, D18112. https://doi.org/10.1029/2010JD013850

Fuller-Rowell, T., Wu, F., Akmaev, R., Fang, T. -W., & Araujo-Pradere, E. (2010). A whole atmosphere model simulation of the impact of a sudden stratospheric warming on thermosphere dynamics and electrodynamics. *Journal of Geophysical Research*, *115*, A00G08. https://doi.org/10.1029/2010JA015524

Garcia, R. R., Smith, A. K., Kinnison, D. E., Cámara, Á. D. L., & Murphy, D. J. (2017). Modification of the gravity wave parameterization in the whole atmosphere community climate model: Motivation and results. *Journal of the Atmospheric Sciences*, *74*, 275–291. https://doi.org/10.1175/jas-d-16-0104.1

Goncharenko, L. P., Chau, J. L., Liu, H.-L., & Coster, A. J. (2010). Unexpected connections between the stratosphere and ionosphere. *Geophysical Research Letters*, *37*, L10101. https://doi.org/10.1029/2010GL043125

Goncharenko, L. P., Coster, A. J., Plumb, R. A., & Domeisen, D. I. V. (2012). The potential role of stratospheric ozone in the stratosphere-ionosphere coupling during stratospheric warmings. *Geophysical Research Letters*, *39*, L08101. https://doi.org/10.1029/2012GL051261

Goncharenko, L. P., Harvey, V. L., Greer, K. R., Zhang, S. R., & Coster, A. J. (2020). Longitudinally dependent low-latitude ionospheric disturbances linked to the Antarctic sudden stratospheric warming of September 2019. *Journal of Geophysical Research: Space Physics*, *125*, e2020JA028199. https://doi.org/10.1029/2020JA028199

Gu, S.-Y., Ruan, H., Yang, C.-Y., Gan, Q., Dou, X., & Wang, N. (2018). The morphology of the 6-day wave in both the neutral atmosphere and F region ionosphere under solar minimum conditions. *Journal of Geophysical Research: Space Physics*, *123*, 4232–4240. https://doi.org/10.1029/2018JA025302

Hagan, M. E., Burrage, M. D., Forbes, J. M., Hackney, J., Randel, W. J., & Zhang, X. (1999). GSWM-98: Results for migrating solar tides. *Journal of Geophysical Research*, *104*(A4), 6813–6827. https://doi.org/10.1029/1998ja900125

Hagan, M. E., & Forbes, J. M. (2003). Migrating and nonmigrating semidiurnal tides in the upper atmosphere excited by tropospheric latent heat release. *Journal of Geophysical Research*, *108*(A2), 1062. https://doi.org/10.1029/2002JA009466

Hibbins, R. E., Espy, P. J., Orsolini, Y. J., Limpasuvan, V., & Barnes, R. J. (2019). SuperDARN observations of semidiurnal tidal variability in the MLT and the response to sudden stratospheric warming events. *Journal of Geophysical Research - D: Atmospheres*, *124*, 4862–4872. https://doi.org/10.1029/2018JD030157

Iimura, H., Fritts, D. C., Janches, D., Singer, W., & Mitchell, N. J. (2015). Interhemispheric structure and variability of the 5-day planetary wave from meteor radar wind measurements. *Annales Geophysicae*, *33*(11), 1349–1359. https://doi.org/10.5194/angeo-33-1349-2015

Jacobi, C., Kürschner, D., Muller, H. G., Pancheva, D., Mitchell, N. J., & Naujokat, B. (2003). Response of the mesopause region dynamics to the February 2001 stratospheric warming. *Journal of Atmospheric and Solar-Terrestrial Physics*, *65*, 843–855. https://doi.org/10.1016/s1364-6826(03)00086-5

Jiang, J. H., Wu, D. L., & Eckermann, S. D. (2002). Upper Atmosphere Research Satellite (UARS) MLS observation of mountain waves over the Andes. *Journal of Geophysical Research*, *107*(D20), 8273. https://doi.org/10.1029/2002JD002091

Jin, H., Miyoshi, Y., Pancheva, D., Mukhtarov, P., Fujiwara, H., & Shinagawa, H. (2012). Response of migrating tides to the stratospheric sudden warming in 2009 and their effects on the ionosphere studied by a whole atmosphere-ionosphere model GAIA with COSMIC and TIMED/SABER observations. *Journal of Geophysical Research*, *117*, A10323. https://doi.org/10.1029/2012JA017650

Kim, J.-H., Kim, Y. H., Lee, C.-S., & Jee, G. (2010). Seasonal variation of meteor decay times observed at King Sejong Station (62.22°S, 58.78°W), Antarctica. *Journal of Atmospheric and Solar-Terrestrial Physics*, *72*(11–12), 883–889. https://doi.org/10.1016/j.jastp.2010.05.003

Krüger, K., Naujokat, B., & Labitzke, K. (2005). The unusual midwinter warming in the southern hemisphere stratosphere 2002: A comparison to northern hemisphere phenomena. *Journal of the Atmospheric Sciences*, *62*(3), 603–613. https://doi.org/10.1175/jas-3316.1

Lee, C., Kim, Y. H., Kim, J.-H., Jee, G., Won, Y.-I., & Wu, D. L. (2013). Seasonal variation of wave activities near the mesopause region observed at King Sejong Station (62.22°S, 58.78°W), Antarctica. *Journal of Atmospheric and Solar-Terrestrial Physics*, *105–106*, 30–38. https://doi.org/10.1016/j.jastp.2013.07.006

Lieberman, R., Riggin, D., Franke, S., Manson, A., Meek, C., Nakamura, T., & Reid, I. (2003). The 6.5-day wave in the mesosphere and lower thermosphere: Evidence for baroclinic/barotropic instability. *Journal of Geophysical Research*, *108*, 4640. https://doi.org/10.1029/2002JD003349

Lieberman, R. S., Oberheide, J., Hagan, M. E., Remsberg, E. E., & Gordley, L. L. (2004). Variability of diurnal tides and planetary waves during November 1978-May 1979. *Journal of Atmospheric and Solar-Terrestrial Physics*, *66*, 517–528. https://doi.org/10.1016/j.jastp.2004.01.006

Lieberman, R. S., Riggin, D. M., Ortland, D. A., Oberheide, J., & Siskind, D. E. (2015). Global observations and modeling of nonmigrating diurnal tides generated by tide-planetary wave interactions. *Journal of Geophysical Research - D: Atmospheres*, *120*, 11419–11437. https://doi.org/10.1002/2015JD023739

Lin, J. T., Lin, C. H., Rajesh, P. K., Yue, J., Lin, C. Y., & Matsuo, T. (2020). Local-time and vertical characteristics of quasi-6-day oscillation in the ionosphere during the 2019 Antarctic sudden stratospheric warming. *Geophysical Research Letters*, *47*, e2020GL090345. https://doi.org/10.1029/2020GL090345

Liu, G., England, S. L., Immel, T. J., Frey, H. U., Mannucci, A. J., & Mitchell, N. J. (2015). A comprehensive survey of atmospheric quasi 3 day planetary-scale waves and their impacts on the day-to-day variations of the equatorial ionosphere. *Journal of Geophysical Research*, *120*, 2979–2992. https://doi.org/10.1002/2014JA020805

Liu, G., Immel, T. J., England, S. L., Kumar, K. K., & Ramkumar, G. (2010). Temporal modulation of the four-peaked longitudinal structure of the equatorial ionosphere by the 2 day planetary wave. *Journal of Geophysical Research*, *115*, A12338. https://doi.org/10.1029/2010JA016071

Liu, G., Janches, D., Lieberman, R. S., Moffat-Griffin, T., Fritts, D. C., & Mitchell, N. J. (2020). Coordinated observations of 8- and 6-hr tides in the mesosphere and lower thermosphere by three meteor radars near 60°S latitude. *Geophysical Research Letters*, *47*, e2019GL086629. https://doi.org/10.1029/2019GL086629

Liu, H.-L., & Roble, R. G. (2002). A study of a self-generated stratospheric sudden warming and its mesospheric-lower thermospheric impacts using the coupled TIME-GCM/CCM3. *Journal of Geophysical Research*, *107*(D23), 15–21. https://doi.org/10.1029/2001JD001533

Liu, H.-L., Talaat, E., Roble, R., Lieberman, R., Riggin, D., & Yee, J. H. (2004). The 6.5-day wave and its seasonal variability in the middle and upper atmosphere. *Journal of Geophysical Research*, *109*, D21112. https://doi.org/10.1029/2004jd004795

Liu, H.-L., Wang, W., Richmond, A. D., & Roble, R. G. (2010). Ionospheric variability due to planetary waves and tides for solar minimum conditions. *Journal of Geophysical Research*, *115*, A00G01. https://doi.org/10.1029/2009JA015188

Matsuno, T. (1971). A dynamical model of the stratospheric sudden warming. *Journal of the Atmospheric Sciences*, *28*, 1479–1494. https://doi.org/10.1175/1520-0469(1971)028<1479:admots>2.0.co;2

Meyer, C. K., & Forbes, J. M. (1997). A 6.5-day westward propagating planetary wave: Origin and characteristics. *Journal of Geophysical Research*, *102*(D22), 26173–26178. https://doi.org/10.1029/97jd01464

Miyoshi, Y. (1999). Numerical simulation of the 5-day and 16-day waves in the mesopause region. *Earth Planets and Space*, *51*(7–8), 763–772. https://doi.org/10.1186/bf03353235

Miyoshi, Y., & Hirooka, T. (1999). A numerical experiment of excitation of the 5-day wave by a GCM. *Journal of the Atmospheric Sciences*, *56*(11), 1698–1707. https://doi.org/10.1175/1520-0469(1999)056<1698:aneoeo>2.0.co;2

Moudden, Y., & Forbes, J. M. (2010). A new interpretation of Mars aerobraking variability: Planetary wave-tide interactions. *Journal of Geophysical Research*, *115*, E09005. https://doi.org/10.1029/2009JE003542

Oberheide, J., Pedatella, N. M., Gan, Q., Kumari, K., Burns, A. G., & Eastes, R. W. (2020). Thermospheric composition O/N response to an altered meridional mean circulation during sudden stratospheric warmings observed by GOLD. *Geophysical Research Letters*, *47*, e2019GL086313. https://doi.org/10.1029/2019GL086313

Pancheva, D., Mitchell, N., Clark, R. R., Drobjeva, J., & Lastovicka, J. (2002). Variability in the maximum height of the ionospheric F2-layer over Millstone Hill (September 1998-March 2000); Influence from below and above. *Annales Geophysicae*, *20*, 1807–1819. https://doi.org/10.5194/angeo-20-1807-2002

Pancheva, D., Mukhtarov, P., & Andonov, B. (2009). Nonmigrating tidal activity related to the sudden stratospheric warming in the Arctic winter of 2003/2004. *Annales Geophysicae*, *27*, 975–987. https://doi.org/10.5194/angeo-27-975-2009

Pedatella, N. M., & Forbes, J. M. (2010). Evidence for stratosphere sudden warming-ionosphere coupling due to vertically propagating tides. *Geophysical Research Letters*, *37*, L11104. https://doi.org/10.1029/2010GL043560

Pedatella, N. M., & Liu, H.-L. (2013). The influence of atmospheric tide and planetary wave variability during sudden stratosphere warmings on the low latitude ionosphere. *Journal of Geophysical Research: Space Physics*, *118*, 5333–5347. https://doi.org/10.1002/jgra.50492

Pedatella, N. M., Liu, H. L., & Hagan, M. (2012). Day-to-day migrating and nonmigrating tidal variability due to the six-day planetary wave. *Journal of Geophysical Research*, *117*, A06301. https://doi.org/10.1029/2012ja017581

Pedatella, N. M., Liu, H.-L., Marsh, D. R., Raeder, K., Anderson, J. L., Chau, J. L., et al. (2018). Analysis and hindcast experiments of the 2009 sudden stratospheric warming in WACCMX+DART. *Journal of Geophysical Research: Space Physics*, *123*, 3131–3153. https://doi.org/10.1002/2017JA025107

Pedatella, N. M., Liu, H.-L., Richmond, A. D., Maute, A., & Fang, T.-W. (2012). Simulations of solar and lunar tidal variability in the mesosphere and lower thermosphere during sudden stratosphere warmings and their influence on the low-latitude ionosphere. *Journal of Geophysical Research*, *117*, A08326. https://doi.org/10.1029/2012JA017858

Preusse, P., Ern, M., Eckermann, S. D., Warner, C. D., Picard, R. H., Knieling, P., et al. (2006). Tropopause to mesopause gravity waves in August: Measurement and modeling. *Journal of Atmospheric and Solar-Terrestrial Physics*, *68*, 1730–1751. https://doi.org/10.1016/j.jastp.2005.10.019

Siddiqui, T. A., Maute, A., & Pedatella, N. M. (2019). On the importance of interactive ozone chemistry in Earth-system models for studying mesophere-lower thermosphere tidal changes during sudden stratospheric warmings. *Journal of Geophysical Research: Space Physics*, *124*, 10690–10707. https://doi.org/10.1029/2019JA027193

Stober, G., Janches, D., Matthias, V., Fritts, D., Marino, J., Moffat-Griffin, T., et al. (2020). Seasonal evolution of winds, atmospheric tides and Reynolds stress components in the Southern hemisphere mesosphere/lower thermosphere in 2019. *Annales Geophysicae*. https://doi.org/10.5194/angeo-2020-55

Teitelbaum, H., & Vial, F. (1991). On tidal variability induced by nonlinear interaction with planetary waves. *Journal of Geophysical Research*, *96*, 14169–14178. https://doi.org/10.1029/91JA01019

Wang, H., Fuller-Rowell, T. J., Akmaev, R. A., Hu, M., Kleist, D. T., & Iredell, M. D. (2011). First simulations with a whole atmosphere data assimilation and forecast system: The January 2009 major sudden stratospheric warming. *Journal of Geophysical Research*, *116*, A12321. https://doi.org/10.1029/2011JA017081

Wu, Q., Ortland, D. A., Solomon, S. C., Skinner, W. R., & Niciejewski, R. J. (2011). Global distribution, seasonal, and inter-annual variations of mesospheric semidiurnal tide observed by TIMED TIDI. *Journal of Atmospheric and Solar-Terrestrial Physics*, *73*, 2482–2502. https://doi.org/10.1016/j.jastp.2011.08.007

Yamazaki, Y. (2018). Quasi-6-day wave effects on the equatorial ionization anomaly over a solar cycle. *Journal of Geophysical Research: Space Physics*, *123*, 9881–9892. https://doi.org/10.1029/2018JA026014

Yamazaki, Y., Matthias, V., Miyoshi, Y., Stolle, C., Siddiqui, T., Kervalishvili, G., et al. (2020). September 2019 Antarctic sudden stratospheric warming: Quasi-6-day wave burst and ionospheric effects. *Geophysical Research Letters*, *47*, e2019GL086577. https://doi.org/10.1029/2019GL086577